Convention Special Issue – 2020

J. Indian Chem. Soc.,
Vol. 97, No. 12a, December 2020, pp. 2553-2565

# Recognition-mediated supramolecular assemblies of 4′,6-diamidino-2-phenylindole (DAPI) with cationic receptors: Modulation in the photophysical properties and prospects†

**Meenakshi N. Shinde[a,$], Jyotirmayee Mohanty*[a,b] and Achikanath C. Bhasikuttan*[a,b]**

[a]Radiation and Photochemistry Division, Bhabha Atomic Research Centre, Trombay, Mumbai-400 085, India

[b]Homi Bhabha National Institute, Training School Complex, Anushaktinagar, Mumbai-400 094, India

[$]Present address: Skaggs School of Pharmacy and Pharmaceutical Sciences, University of California, San Diego, 9500 Gilman Drive MC 0751, La Jolla, CA 92093-075.

*E-mail:* jyotim@barc.gov.in, bkac@barc.gov.in

*Manuscript received online 01 November 2020, revised and accepted 30 December 2020*

Supramolecular assemblies through noncovalent host-guest complexation have gained enormous research interests for the creation of custom designed smart materials having different functionalities due to the alteration in the molecular properties of the guests. This mini-review provides an account on the recognition-mediated changes/modulations in the photophysical aspects of a bio marker, 4′,6-diamidino-2-phenylindole (DAPI), with three cationic receptors, *p*-sulfonatocalix[6]arene (SCX6), cucurbit[7]uril (CB7) and sulfobutylether β-cyclodextrin ($SBE_7\beta CD$). Though all the three macrocyclic hosts are cationic receptors and having the similar cavity dimension, DAPI exhibits distinctly different photophysical properties with each host molecules as the chemical constituent of the hosts are entirely different. These interesting host-guided fluorescence response and the modified/improved photophysical properties of complexed DAPI with different cavitands can be utilized for various applications such as fluorescent pH sensor, stimuli-responsive on-off switch, detection of biomolecules, etc.

Keywords: *p*-Sulfonatocalix[6]arene, sulfobutylether β-cyclodextrin, cucurbit[7]uril, 4′,6-diamidino-2-phenylindole, host-guest complex.

## 1. Introduction

Supramolecularly functionalized assemblies have shown upsurge in the current research interests owing to their potential applications as nanoreactors[1], enzymatic assay[2], turn-on turn-off fluorescence sensors[3,4], aqueous dye laser[5,6], drug delivery[7,8], molecular switches[9,10], in catalysis[11], etc. In this regard, construction of supramolecular assemblies through noncovalent host-guest interaction are being projected as the suitable/facile strategy in contrast to the conventional synthetic methods because such assemblies respond to external stimuli in controlled and quantitative manners, so that one can tune the intrinsic molecular properties of the guest in the desired ways[12,13]. One of the major interests in supramolecular assemblies is the design of structurally well-defined architectures with dynamic and stimulus-responsive properties. Dynamic and adaptive supramolecular assemblies created from smaller molecular building units find several applications in materials and medicines. In this regard, various supramolecular systems involving preorganized synthetic receptors such as crown ethers, calixarenes, cyclodextrins and more recently cucurbiturils have been documented in the literature[14,15].

The supramolecular hosts such as cyclodextrins, calix[*n*]arenes, or cucurbit[*n*]urils are well known to act as molecular container of different geometrical confinement and microenvironment such as anionic, cationic or neutral forms, to yield host-guest complexes, thereby, modulating chemical properties of the guest[14,16]. The host-guest complexes are mainly driven by weak and reversible noncovalent interactions such as hydrogen bonding, ion-dipole, π-π stacking and van der Waals forces. The host encapsulated guest is isolated from the aqueous bulk which subsequently enhances

†**Invited Lecture.**

thermal as well as photochemical stability of a guest in the course of preventing bimolecular reactions[14,17,18]. Especially, the hydrophobic guest molecule may show enhanced solubility and stability in the presence of host. Also, the stoichiometries of host-guest complex formed show pronounced effect on the photophysical properties of guests/dyes, such as formation of monomer, dimer/excimer or aggregation[9,12,19,20]. Formation of these host-guest stoichiometries can be controlled by virtue of external stimuli like pH, salt, light and by addition of other competing guests[1,20–22]. The change in fluorescence behavior of dyes upon host-guest complexation provides an excellent scholastic example of recognition-mediated fluorescent assemblies, having vast utilities in fluorescence sensing[3,4], on-off switches[9], controlled drug uptake/release[7,8], enzymatic assay[2], nanocapsules[1], photo-stabilization[17,18], supramolecular catalysis[11], supramolecular architectures[23] and aqueous dye laser[5,6,24].

The fluorescence of organic/inorganic dyes is sensitive to their environment; also it can be manipulated by the steric stress on rotation of particular bond and it is applied to wide range of problems in the chemical and biological sciences. Of all biological staining agents, 4′,6-diamidino-2-phenylindole (DAPI) is most explored by virtue of its photophysical properties in the presence of biomolecules[25–29]. Scientists have taken a lot of efforts to pinpoint the DAPI's equivocal fluorescence, among which the first report was published by A. G. Sazbo *et al*. in 1986[30] wherein they have carried out pH dependent fluorescence study of DAPI and suggested that, the fast intramolecular proton transfer in the singlet excited state to the indole ring is the main cause for the poor emission yield of DAPI in solution[30]. They also proposed that the prevention of intramolecular proton transfer led to enhanced quantum yield with blue emission of DAPI in the DNA strands. Similar efforts have been carried out by E. Gratton *et al*.[31] and they have shown that DAPI exists in "two ground state conformers" (Fig. 1). The fluorescence of DAPI in the 415–520 nm range is originated from two different ground sate conformers, one of them having lifetime ~0.13 ns (97%) which is planar and quenched by water mediated proton transfer at NH of indole ring and the other conformer twisted with lifetime of about ~1.74 ns (3%)[28,30–32]. The percentage of the slow decay component reduced when the monitoring region was changed towards red and its contribution disappeared beyond 550 nm. In recent years, the modulation of the photophysical properties and the restriction in the proton transfer behavior of DAPI in the presence of three cation receptors, namely, *p*-sulfonatocalix[*n*]arene (*n* = 4 and 6), cucurbit[7]uril and sulfobutylether derivative of β-CD ($SBE_7$βCD) have been reported[21,33,34].

*1.1. Macrocyclic host molecules:*

In the last several decades various natural and synthetic cavitand host molecules have been reported for selectively binding to metal cations. Among these host molecules, the non covalent host-guest interactions of cyclodextrins,

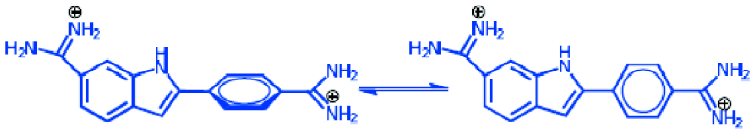

**Fig. 1.** Two conformers of 4′,6-diamidino-2-phenylindole (DAPI).

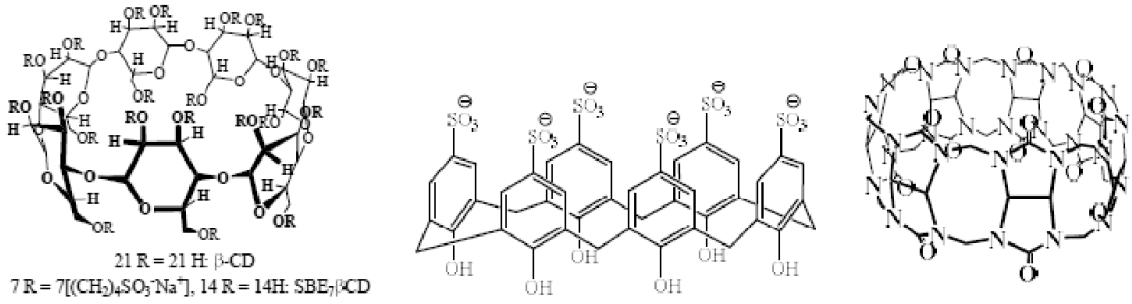


**Fig. 2.** Chemical structures of sulfobutylether β-cyclodextrin, *p*-sulfonatocalix[6]arene and cucurbit[7]uril.

calixarenes, and cucurbiturils (Fig. 2) have been studied extensively[35].

*Cyclodextrins:*

Cyclodextrins (CDs), the naturally occurring cyclic oligomers α-, β-, and γ-CD, composed of 6, 7, and 8 α-D-glucose units, respectively, are the most classical example of cavitand macrocyclic moieties that have been extensively studied for the noncovalent host-guest interaction with fluorescent dyes[36]. They are uncharged truncated cone of hydrophobic inner cavity with lower and upper rim of hydrophilic hydroxyl groups[37], which affords added hydrogen bonding centers for the interaction of guest molecules. The binding constants of CDs are usually ~10 to $10^5$ $M^{-1}$ and hence mM concentrations of the host is required to achieve nearly complete complexation[38,39]. Though the cyclodextrins and their complexes are hydrophilic, their solubility in aqueous medium is relatively sparse, especially that of β-cyclodextrin, which is about 16 mM[15,35]. There are various kind of substituted CDs reported till this date to accomplish deeper hydrophobic cavities, reduced toxicity and/or to improve guest binding via improved ionic, ion-dipole, as well hydrophobic interactions. Sulfobutylether β-cyclodextrin ($SBE_7$βCD, marketed as Captisol) is nothing but a modified β-cyclodextrin derivative, where 4 > OH alcoholic groups in the larger rim and 3 alternate primary alcoholic groups (-OH) in the smaller rim of β-CD are replaced by sulfobutylether arms (Fig. 2)[33,40,41]. Note that $SBE_7$βCD posses the hydrophobic interior of β-cyclodextrin with $SO_3^-$ terminated alkyl chains. This allows the hydrophobic cavity to interact with cationic guests through their negatively polarized/charged extended portals and more importantly it increases the aqueous solubility of $SBE_7$βCD to about 70 g/100 ml at 25°C and is remarkably higher than the β-CD, which is only about 1.85 g/100 ml at 25°C[40]. Recenly, we have demonstrated $SBE_7$βCD-assisted inhibition of protein fibrillation and its disintegration[42]. In other studies we have established the aqueous dye laser system with $SBE_7$βCD-encapsulated rhodamine dyes[5] and supramolecular photosensitizer with $SBE_7$βCD-complexed porphyrin[43]. Of late, the $SBE_7$βCD-complexed thiazole orange has been employed for the detection of neurotransmitter tyramine[44] and the enhanced antibacterial activity of sangunarine drug has been achieved in the presence of $SBE_7$βCD[45].

*Calix[n]arenes:*

The calix[*n*]arenes (CXs) having cavity sizes of *n* = 4, 6, and 8 are product of single step base-catalyzed condensation of 4-substituted phenols with formaldehyde linked by methylene bridges at the meta-positions[46]. The poor water solubility of calixarenes led to the development of several derivatized calixarenes prepared by modifying the portal functional groups which also provided distinct selectivity for a particular guest. The sulfonated analogues, synthesized by Shinkai *et al.*, are the most intensively studied water-soluble CXs[47]. *p*-Sulfonatocalix[*n*]arene (*n* = 4–8; SCXn) have received immense attention in the area of sensors, ion-sensitive electrodes, enzyme mimetics, antibacterial, antiviral, membrane selectives, nonlinear optics etc.[3,48,49]. In our recent studies, SCXn and their complexes have been used as fibril inhibitor, fluorescence-based pH sensor, off-on switch, ratiometric sensing, capping agent for the synthesis of silver nanoparticles and in drug delivery applications[21,50–54].

*Cucurbit[n]urils (CBs):*

The methylene-bridged glycoluril monomers come together to form a cyclic oligomer called cucurbit[*n*]urils possessing a hydrophobic interior having entry through the symmetrical carbonyl laced portals[15,16,55–57]. Based on the number of monomer units joined, a series of cucurbit[*n*]urils (CBn; *n* = 5–10) having different cavity and portal sizes are reported. The CBs have been proved as proficient hosts which can bind to wide range of guests, such as metal ions or alkyl or arylamine (protonated) through carbonyl portals via ion-dipole interactions and to aromatic organic dyes through their cavities via hydrophobic forces. Whereas the electron deficient carbon centers at the peripheral region shows interaction with polyanions[58]. The binding constants of CB host-guest complexes ranges from $10^4$–$10^{15}$ $M^{-1}$ and on that front they are famous to compete with natural self-assemblies like avidin-biotin ($K_b$ = $10^{15}$ $M^{-1}$)[59]. Among CBs, CB7 has attested itself as the most promising host molecule for variety of fluorescent guest dyes, due to its favorable cavity size and more water solubility (~5 mM)[15,16] than the other CBs. The CBs impacted a wide variety of scientific research areas due to their versatile ability to form binary and ternary host-guest complexes. Nau *et al.*[60] and Isaacs *et al.*[61] proved independently that CBs present low *in vivo* and *in vitro* toxicity, thus enabling several applications in biological systems. Several reviews are dedicated to the synthesis, host-guest binding properties of CBs and application in drug delivery, catalysis, sensors and stimuli responsive self-assembly[14,15,55–57,62–64].

The CBs are known as cationic receptor and hence can also discriminate between cationic/neutral forms of guest enabling efficient control over prototropic equilibrium between protonated and deprotonated form of dyes[65]. This control over prototropic equilibrium has resulted in pronounced $pK_a$ shifts of drug molecules along with solubility, stability, bioavailability enhancement and demonstrated as useful strategy for drug delivery application[7,35,66]. Of late the use of CBs as capping agent to nanoparticles has craved scientist's attention[13,67,68].

In this review article, we have discussed the interaction of DAPI with three macrocyclic hosts, namely, *p*-sulfonatocalix[6]arene (SCX6), sulfobutylether derivative of β-CD ($SBE_7\beta CD$), and cucurbit[7]uril (CB7) having similar cavity dimensions and elaborated on the utilization of the host assisted altered molecular properties of DAPI for applications such as fluorescence sensor, drug delivery applications.

## 2. Interaction of DAPI with macrocyclic hosts

The complexation between host and guest molecules through noncovalent interaction modulates the molecular properties of the guest significantly. As a result, the ensued supramolecular assemblies show different functionalities which can be employed for various applications. The spectacular changes in the photophysical behavior of DAPI with SCX6, $SBE_7\beta CD$ and CB7 hosts and the promising applications of the said supramolecular assemblies of DAPI have been briefly discussed in the following sections.

### *2.1. Interaction of DAPI with p-sulfonatocalix[6]arene:*

#### *2.1.1. Effect of SCX6 encapsulation on the absorption/ fluorescence behavior of DAPI:*

The dicationic dye (DAPI) in water displays an absorption spectrum having spectral bands in the 300 nm–400 nm region with the absorption maximum centered ~342 nm[69]. Since, the first protolytic equilibrium ($pK_{a1}$) of SCX6 occurs at ~3.4[70], the interaction between SCX6 and DAPI has been investigated at two pH conditions (2.5 and 6) of the solution. On titration of the DAPI solution (at both the pHs; 2.5 and 6) with SCX6 host, presented notable changes in the absorption spectral features. The absorption displayed a hypochromic behavior in the region below 300 nm, whereas, in effect, the absorption profile resulted in ~10 nm red shift[21]. All these changes occurred smoothly with neat isosbestic points, one ~371 nm (for pH 2.5 solution) and the other ~376 nm (for the solution at pH 6), characteristic of complex formation among the host SCX6 and the guest DAPI.

Modulations in the photophysical properties of DAPI upon complexation with SCX6 were critically analyzed from the variations in the emission features at the preset solution pHs. In a dilute solution of DAPI (5 μM, pH 6) rendered emission bands in the 400 nm to 650 nm region with the intensity maximum ~480 nm. Addition of SCX6 to the above solution led to drastic decrease in the emission intensity and the emission maximum blue shifted to 457 nm[21]. As reported, CXn and its other derivatized compounds are well established as excellent electron donors[51,71–73]. Due to this feature, they competently interact with the excited state of DAPI through electron transfer leading to the observed quenching of emission intensity[73].

On the other hand, maintaining the solution pH at 2.5 there by allowing the $SO_3^-$ groups to exist in solution along with undissociated phenolic -OH groups, the interaction of SCX6 led to a striking increase in the emission intensity to ~6-fold as monitored at ~480 nm along with a shift in the emission maximum to 466 nm. In terms of quantum yield, the comparison of the area under the emission profile of the complex and with the reported value of DAPI alone in water ($\phi_f = 0.04$)[32], the emission yield of the SCX6-DAPI complex at pH 2.5 was evaluated to be 0.26. This is in good agreement with the 6 fold enhancement value arrived from the intensity measurement at a single wavelength as well. Further, the spectral shift towards blue region is understood as the dipole of DAPI (complexed with SCX6) in the excited state is less stabilized as the host cavity renders a less polar microenvironment as compared to the aqueous medium[25].

The above striking changes in the fluorescence behaviour at pH 2.5 and pH 6 notify that the binding of DAPI with SCX6 at these pHs are differently placed. On the basis of very low $pK_a$ of $-SO_3H$ (< 1), it is understood that at pH 2.5 the $-SO_3H$ groups at the upper portal will remain as $SO_3^-$ and the phenolic -OH groups at the bottom portal remain in its undissociated -OH form. Here, it is possible that DAPI prefers an inclusion complex formation through axial binding (vertical) or a top stacking (horizontal stacking) through the top portal of SCX6. This will impart DAPI more rigidity and planarity there by increasing the radiative emission yield. However at pH 6, some of the phenolic -OH groups also exists as deprotonated and the ensuing phenolate anions are stabilized by forming an intra-molecular hydrogen bonded structure at the lower

portal[70,74]. It is believed that the possible collective proton motion in the intramolecular hydrogen bonding network causes an enhanced polarizability of the phenolic protons in SCX6[74]. This feature may support other excited state pathways such as electron transfer etc. So the chemistry at pH 6 in the SCX6-DAPI system suggests that at pH 6, DAPI is placed close to the lower rim -OH/$O^-$ groups. This arrangement will assist an electron transfer interaction which will bring down the emission intensity as observed in the experiments at this pH[21]. The binding constants ($K_{eq}$) for the interaction of DAPI and SCX6 at the preset pH conditions (pH 2.5 and pH 6) have been obtained from the nonlinear fitting parameters of the binding curve constructed from emission intensity variations[75]. The binding constants values thus obtained following a 1:1 stoichiometric composition were ~4.5×$10^6$ $M^{-1}$ and ~4.5×$10^4$ $M^{-1}$ respectively at pH 6 and pH 2.5.

*2.1.2. pH induced modulations in the fluorescence properties of SCX6-DAPI complex:*

Following the published reports[70] it is tough to evaluate the accurate p$K_a$ of sulfonatocalixarenes by the instrumental methods as question arises due to the strongly acidic calixarene portal -OH groups in combination with the presence of interfering dissociation of -$SO_3H$ groups. Taking advantage of the supramolecular route in addressing this issue, the modulations in the emission profile of the SCX6:DAPI complex with the change in solution pH was examined. As presented in Fig. 3, the emission intensity of the complexed dye steadily diminished with a corresponding increase in the pH of the SCX6-DAPI system. The details of the emission intensity variations monitored at 480 nm (shown in the inset of Fig. 3) displayed a sigmoidal $pK_a$ curve. From a suitable analysis of this $pK_a$ curve[21], the $pK_a$ was found to be 3.45, and is close agreement with the known $pK_1$ of SCXn[70].

*2.1.3. Changes in the fluorescence lifetime and anisotropy of DAPI in presence of SCX6:*

Structurally DAPI in water exists in two conformational structures. In one case, it maintains planarity with the benzene and indole groups in one plane and this major planar form (~97%) diplays a lifetime of ~0.13 ns. In the second case, the benzene ring remain twisted against the indole group and this conformer having a minor contribution (~3%) exhibits lifetime ~2 ns[25,69]. Since the indole nitrogen is available for the hydrogen bonding interaction with the water molecules, photoexcitation leads to effective protonation of this indole nitrogen. This excited state protonation reaction strongly quench the emission intensity of DAPI and esults in the display of fast fluorescence decay with a lifetime of 0.13 ns[25,69]. However, on the other hand, the twisted form experiences a steric restriction in maintaining the hydrogen bonding and does not undergo solvent supported protonation reaction. For this reason, this minor form exhibits longer fluorescence lifetime of about 2 ns[25,69]. Measurements on the SCX6 complexed DAPI at pH 2.5 revealed that the fluorescence decay became slower and ~26% amplitude displayed ~15 ns component in presence of ~20 μM of SCX6 host. This change is readily understood as the rigidization of DAPI dye on complexation with SCX6 host brings out restrictions on the torsional motions of DAPI bonds and hence the excited state protonation channel is severely affected. This will, on the other hand, reduce the non radiative pathway realizing longer relaxation time for the excited state of DAPI as recorded[21].

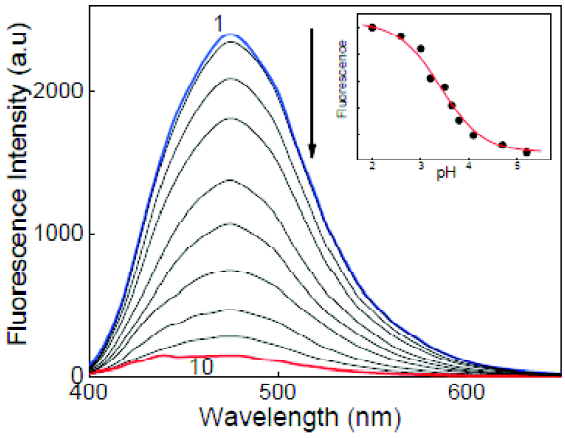


**Fig. 3.** Fluorescence profile of DAPI (~5 μM) in aqueous solution having 250 μM SCX6 at pHs: (1) 2, (2) 2.6, (3) 3, (4) 3.2, (5) 3.5, (6) 3.65, (7) 3.8, (8) 4.1, (9) 4.7 and (10) 5.2. Inset shows the changes in the fluorescence intensity of DAPI at 480 nm in the presence of 250 μM SCX6 with regular change in pH in the range 2 to 6. $\lambda_{ex}$ = 370 nm.

However, the excited state decay time of DAPI-SCX6 complex at pH ~6 could not be measured conveniently as the emission intensity decreased due to the strong quenching and the ensuing short lifetime. This strong fluorescence quenching further points to a newer relaxation pathway for the excited state of DAPI in presence of SCX6 at pH 6. Here

we may recall that the calixarenes in general, are known as good electron donors[71–73] and the photoexcited state of DAPI may act as good electron acceptor[76]. This combination can lead to an effective electron transfer from the SCX6 phenolate moieties to DAPI realizing the severe emission quenching and the fast excited state decay profiles.

Fluorescence methods, especially the time dependent fluorescence anisotropy measurements give valuable data on the molecular volume (hydrodynamic) of the fluorescing moiety. The information on the volume thus allows the calculation of size and hence the geometrical changes due to complexation. In principle, the experimentally obtained rotational correlation time ($\tau_r$), of the emitting species is connected to its rotational diffusion coefficient ($D_r$) according to the Stokes-Einstein relationship[77]. As expected it was seen that DAPI with the host SCX6 at pH 2.5, provided $r_0$ value as 0.25 and the decay traces followed a mono-exponential kinetics, with a $\tau_r$ = ~0.44 ns[21]. The decrease in $\tau_r$, explains the strong complex formation and the placement of DAPI in the cavity of SCX6, acknowledging the molecular rigidity and the enhanced molecular volume of the dye.

*2.2. Interaction of DAPI with sulfobutylether β-cyclodextrin (SBE$_7$βCD):*

*2.2.1. Effect of SBE$_7$βCD encapsulation on the absorption and fluorescence behavior of DAPI:*

On titration of the DAPI solution with SBE$_7$βCD host resulted in the decrease in the absorbances in the spectral region below 350 nm and the corresponding spectral changes displayed a red shift of the absorption maximum by ~8 nm. These spectral changes also displayed a clear isosbestic crossover point at 360 nm (Fig. 4A) and the interaction attained a saturation with 160 μM SBE$_7$βCD for a DAPI concentration 5 μM[33]. The strong interaction among SBE$_7$βCD and DAPI is reasonable as the cationic DAPI dye would find strong electrostatic attraction with the -$SO_3^-$ laced extended chains at both the portals of SBE$_7$βCD. The absorptions changes were further followed to examine the stoichiometric composition by constructing a Job plot. The optical density of the dye at 340 nm against the mole fraction of SBE$_7$βCD ($\eta_{SBE_7\beta CD}$) or DAPI ($\eta_{DAPI}$) (Fig. 4B) presented a maximum at 0.5 of mole fraction of $\eta_{DAPI}$, pointing to a 1:1 stoichiometry for the interaction of SBE$_7$βCD with DAPI[33]. In similar line, the fluorescence features of DAPI also presented notable differences in presence of SBE$_7$βCD and are displayed in Fig. 5A. With SBE$_7$βCD the emission intensity increased ~50-fold along with a shift in the emission maximum towards blue region by ~30 nm. Aptly such huge enhancements have been attributed to the rigid encapsulation into the host cavity and also the hydrophobic cavity of the host where the probe experiences a non-polar environment due to the long -$SO_3^-$ bearing butyl chains at both sides, both of which reduces several nonradiative relaxation pathways[16–19]. The enhancement has been quantitatively calculated as emission quantum yield and is found to be quite significant as 24-fold[32]. Interestingly, under similar conditions, the parent cyclodextrin cavity (β-CD) provided only 2-fold enhancement in the emission yield (Fig. 5B). Thus the above evidence points to the competent inclusion complex formation of DAPI within the SBE$_7$βCD cavity.

The spectroscopic changes noted above have also been used to evaluate the binding parameters. Following a 1:1

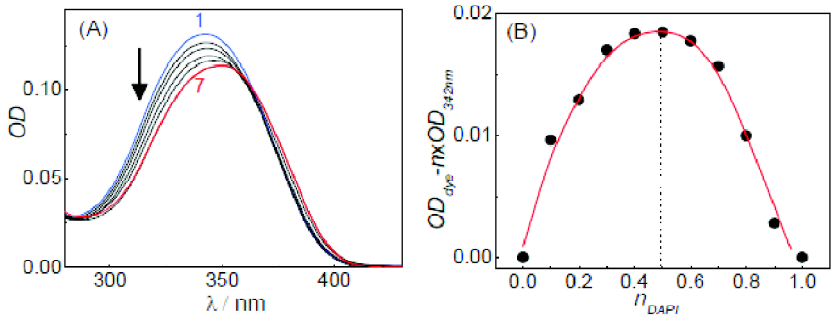


**Fig. 4.** (A) Changes in the absorption spectra of DAPI (~5 μM) in aqueous solution with [SBE$_7$βCD]/(μM): (1) 0, (2) 1, (3) 2, (4) 5, (5) 12, (6) 60, (7) 160. (B) Job's plot generated from the absorbances at 340 nm for the SBE$_7$βCD-DAPI complex. $n_{DAPI}$ is the mole fraction of DAPI. Reproduced with permission from Ref. [33], copyright (2015) John Wiley and Sons.

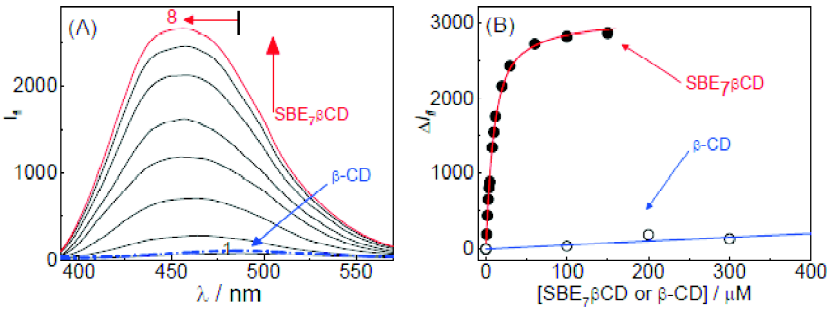


**Fig. 5.** (A) Fluorescence profile of DAPI (5 μM) in aqueous solution with [$SBE_7$βCD]/(μM): (1) 0 (blue line), (2) 1, (3) 3, (4) 6, (5) 10, (6) 20, (7) 40, (8) 160 (red line). (B) Fluorescence intensity changes ($\Delta I_{fl}$ vs [$SBE_7$βCD or β-CD]$_0$ plot) for DAPI-$SBE_7$βCD at pH 6. Filled and open circles are the experimental data points and the solid line is the non linear fit. Reproduced with permission from Ref. [33], copyright (2015) John Wiley and Sons.

composition analysis of the emission intensity changes the value of $K_{eq}$ for the complexation of $SBE_7$βCD with DAPI has been estimated to be (1.4±0.05)×$10^5$ $M^{-1}$ [33]. The strength of the binding interaction is evident when this value is compared with that of the binding constant of DAPI with β-CD as 130 $M^{-1}$ [69]. These results, on the other hand, manifest the importance and utility of custom derivatization of the macrocyclic host to tune the noncovalent interactions for desired applications.

*2.2.2. Excited-state lifetime and fluorescence anisotropy of DAPI; modulations by $SBE_7$βCD interaction:*

The finger prints of the host-guest interactions have also seen in the time dependent excited state parameters as well. The excited state decay profile of DAPI monitored at 480 nm has been recorded in the absence (Fig. 6A (a)) and presence of $SBE_7$βCD (Fig. 6A (b) and (c)). The biexponential traces of DAPI having 0.13 ns (97%) and 2 ns (3%) lifetime values got modified significantly on the addition of $SBE_7$βCD with the appearance of a 3 ns lifetime as the major component. Significant effect on the fast decay component was also seen (0.13 ns to ~1 ns), even on the use of 10 μM of $SBE_7$βCD host. As discussed in the case of calixarenes, the strong effect revealed in the lifetime parameters throw light on the geometrical rigidization due to complexation interaction which hamper the easily feasible nonradiative channels. This host induced restrictions also forbid the excited state proton transfer interaction as well, thus revealing a longer excited state lifetime features[33]. Note that there was no change in the fluorescence traces in the absence and presence of β-CD, understandably due to the absence of any ion-dipole or hydrogen bonding interactions Fig. 6A (c).

The time resolved anisotropy obtained for $SBE_7$βCD-

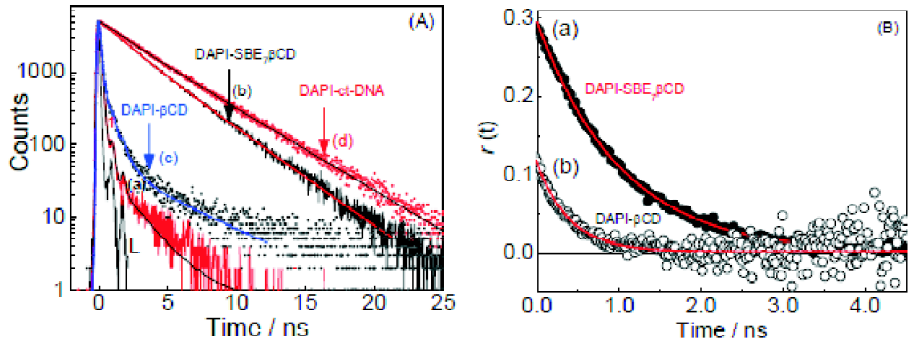


**Fig. 6.** (A) Fluorescence decay profile of DAPI in aqueous solution (a), with 0.3 μM (b) and 160 μM (c) of $SBE_7$βCD, with 5 mM β-CD (d) and with 250 μM of ct-DNA (e). $\lambda_{ex}$ = 374 nm, $\lambda_{em}$ = 480 nm and L represents the lamp profile. (B) Time-resolved fluorescence anisotropy traces of DAPI in the presence of 160 μM $SBE_7$βCD (**a**) and 12 mM β-CD (**b**) in water. Reproduced with permission from Ref. [33], copyright (2015) John Wiley and Sons.

DAPI system (Fig. 6B (a)), provided a $r_0$ value of 0.3 with the decay fit to a monoexponential kinetics with a rotational correlation time constant of $\tau_r$ ~1.2 ns[33]. Contrastingly, the DAPI complex with β-CD (Fig. 5B (b)) rendered the $r_0$ value as ~0.1 and decay fit to a faster kinetics with $\tau_r$ = ~0.41 ns[69]. The difference in the values in these host systems are significant and directly brings out the features of the extended portal substitutions placed on β-CD portals for better encapsulation, stronger interaction and useful spectroscopic properties.

*2.2.3. $^1$H NMR studies on the complex:*

$^1$H NMR study gives information about the complex formation and the interaction sites by monitoring the differences in the chemical shifts of the proton signals of the guest as well as the host molecules. Fig. 7 presents the $^1$H NMR spectra for DAPI alone and also in the presence of $SBE_7$βCD host. A close look at the specific downward chemical shifts of certain proton signals (0.14–0.17 ppm for $H_a$, $H_e$ and $H_f$) and nominal (~0.06 ppm) downfield shifts in the $H_b$, $H_c$ and $H_d$ signals were seen corresponding to the the placement of DAPI within the $SBE_7$βCD cavity and is schematically shown in the inset of Fig. 7(b)[33]. Such total cavitation of DAPI (molecular length ~14–15 Å)[69] in the host cavity is sure to get restrictions on its torsional/conformational movements, leading to the observed enhancement in the photophysical features of DAPI.

*2.2.4. Stimuli-responsive revival of fluorescence emission:*

The above established *'fluorescence turn on'* of the $SBE_7$βCD-DAPI complex was further studied to achieve its stimuli responsive breakage for a '*fluorescence turn off*' condition (Fig. 8a)[33]. This interaction is effected by targeting the sulfonate portals by bringing in a competitive guest. For this, standard analytes such as DNAs, metal-ions or trace analytes of particular significance were employed. The aim was readily achieved with $Ca^{2+}$, which steadily diminished the emission intensity of the complex at 460 nm as in Fig. 8b, trace 1. Moreover, the absorption/emission spectral features were also appeared in reverse to that of the initial complexation changes verifying the dissociation of the complex[33]. Even as the DAPI emission provide *turn on* on the addition of $SBE_7$βCD as in Fig. 8a, the system required 800 mM of $Ca^{2+}$ to establish almost 100% dissociation[33]. This titration also allowed the estimation of the binding constant of $Ca^{2+}$ with $SBE_7$βCD as $1.03\times10^3$ $M^{-1}$ (Fig. 8b, trace 1). Similarly the adamantylamine (AD), has also been studied for the dissociation (Fig. 8b, trace 2) and the estimated binding value obtained was $8.4\times10^3$ $M^{-1}$, much higher than that of $Ca^{2+}$ [33]. Thus with AD, the disassembly was effective with ~26 mM of AD. This stimuli responsive interaction is found to be directly relevant in drug delivery vehicle/drug formulation and therapeutics[78].

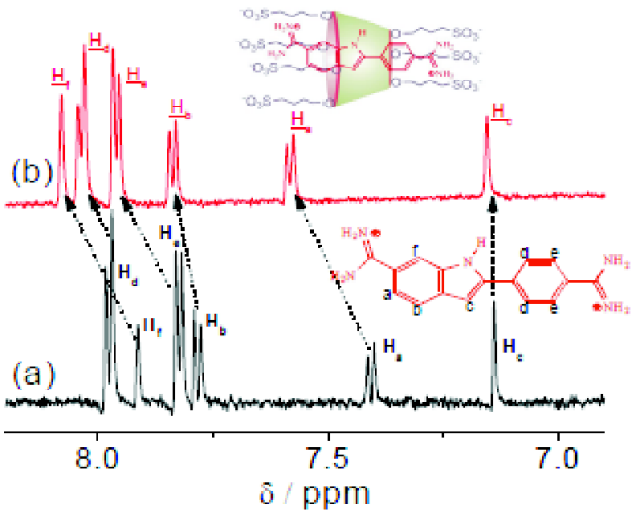


**Fig. 7.** $^1$H NMR (600 MHz) of 100 μM DAPI in the absence (a) and in the presence (b) of $SBE_7$βCD in $D_2O$. Reproduced with permission from Ref. [33], copyright (2015) John Wiley and Sons.

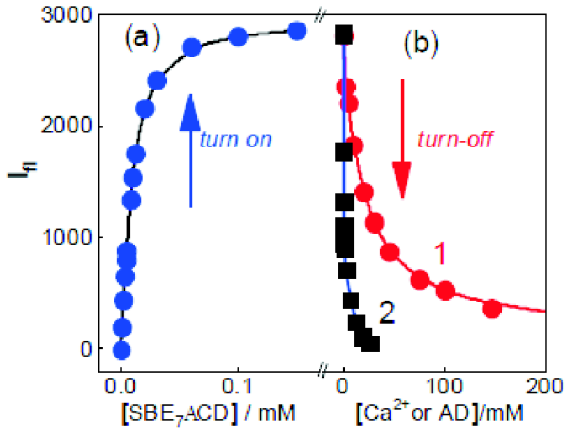


**Fig. 8.** Plot of the emission intensities recorded at 460 nm for DAPI with the addition of (a) $SBE_7$βCD and (b) followed by the addition of $Ca^{2+}$ (1) and AD (2). Reproduced with permission from Ref. [33], copyright John Wiley and Sons.

*2.3. Interaction of DAPI and cucurbit[7]uril (CB7) macrocycle:*

*2.3.1. Consequence of CB7 encapsulation on the absorption/emission behavior of DAPI:*

The absorption band of DAPI shows bathochromic shift along with hypochromic shift upon titration with CB7 and the changes are presented in Fig. 9A. The absorption changes monitored at 320 nm and 385 nm are with CB7 concentration are also presented in the inset of Fig. 9A[34]. From this, the binding constant estimated for 1:1 complex formation was found to be $1.2\times10^7$ $M^{-1}$. DAPI exhibits noteworthy emission increase in presence of CB7 along with a hypsochromic shift in the emission maximum from 496 nm to 468 nm (Fig. 9B) and points to the fact that DAPI experiences a more non polar environment in the CB7 cavity[34]. Nonlinear curve fitting of this fluorescence intensity changes versus CB7 concentrations (inset of Fig. 9B) rendered the binding constant as $1.1\times10^7$ $M^{-1}$ and is in match with the value obtained from absorption measurements. Corresponding changes in the excited state lifetime properties have also been observed and the decay traces of DAPI were found to be changed considerably in presence of CB7. The biexponential decay of DAPI in water became monoexponential with a lifetime of ~1.6 ns when CB7 was added to the system[34]. In line with the lifetime features observed for the other macrocyclic systems, this finding convey that inclusion in to the CB7 cavity disrupts the chances of protonation at the indole nitrogen and hence avoid the presence of different conformers in solution as observed for the free DAPI. It may be noted here that DAPI displayed a shorter lifetime value in CB7 as compared to the 2.6 ns observed in methanol/ethanol solutions[79]. This is understood as the inclusion does not mask DAPI completely from interacting with outside cavity water molecules.

*2.3.2. DAPI-CB7 interaction in the presence of ionic liquids:*

Ionic liquids (ILs) are recently gaining importance as green solvents and hence pose alternative to traditional organic media. In this context, the importance of macrocyclic interaction of one of the ILs, namely, 1-butyl-3-methylimidazolium chloride ($C_4$MImCl) with CB7:DAPI complex for drug delivery applications has been discussed in this section. Fig. 10A shows the changes observed in the absorption profile of CB7-DAPI system in the presence of $C_4$MImCl. Note that the changes were reversed and are in the direction opposite to that recorded in Fig. 9A. This points to the dissociation of the DAPI-CB7 complex by $C_4MIm^+$ cation leading to free DAPI[34]. The steady decrease of emission intensity and the red shift of the emission band (Fig. 10B) indicate a competitive bind-

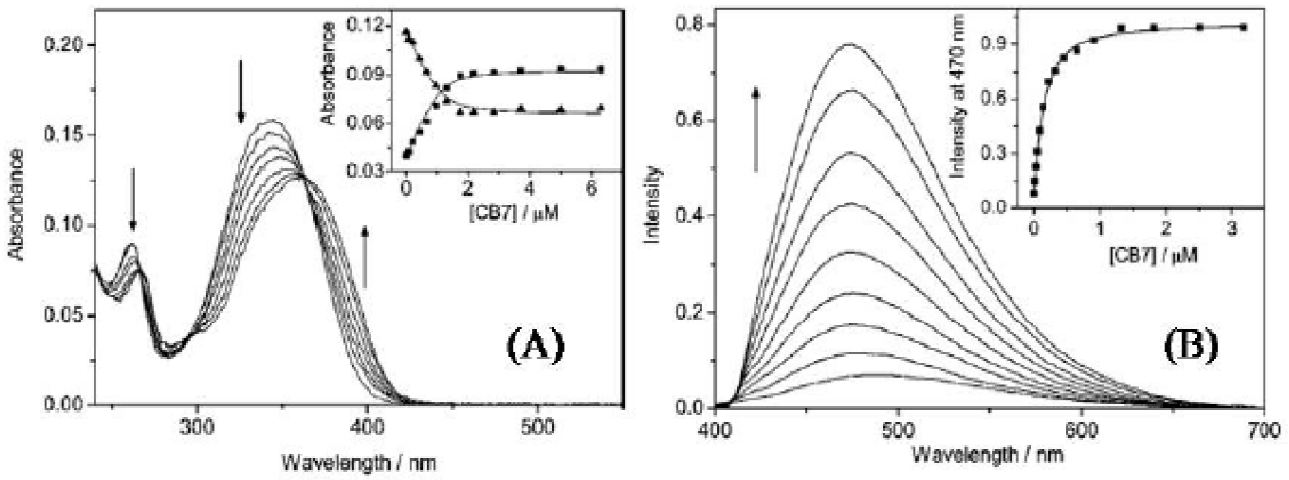


**Fig. 9.** (A) Ground state absorption profile of 1.17 μM DAPI in water in the presence of 0, 0.22, 0.44, 0.66, 0.97, 1.32, and 1.75 μM CB7 in water recorded in a quartz cuvette of 5 cm optical path. Inset displays the absorbance change with CB7 concentration at 320 (decreasing trace) and 385 nm (increasing trace); the line refers to the result of the global fit in the 250–440 nm range. (B) Variation of the fluorescence spectrum of 0.115 μM DAPI aqueous solution on addition of 0, 0.012, 0.029, 0.052, 0.086, 0.141, 0.219, 0.648, and 3.18 μM CB7; excitation at 361 nm. Insert: CB7 concentration dependence of the fluorescence intensity at 470 nm; the line represents the result of the global analysis in the 430–670 nm range. Adapted with permission from Ref. [34], copyright (2009) American Chemical Society.

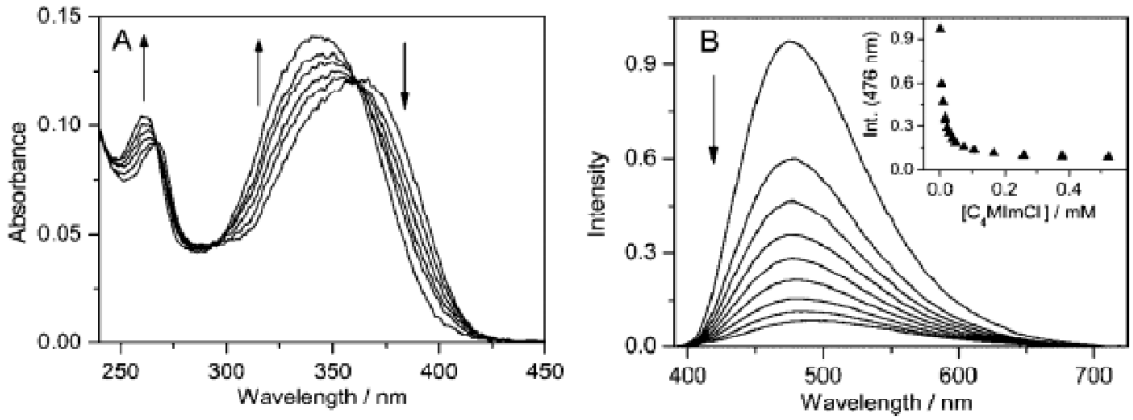


**Fig. 10.** (A) Absorption spectra of 0.91 μM DAPI and 11.3 μM CB7 in aqueous solution in the presence of 0, 18, 27, 45, 68, and 288 μM $C_4MImCl$ at 5 cm optical path. (B) Changes in the fluorescence profile with the addition of 0, 4.6, 9.2, 16, 23, 39, 74, 167, 794 μM $C_4MIm^+Cl^-$ to 4.59 μM DAPI and 2.55 μM CB7 solution; excitation at 361 nm. Inset: Fluorescence intensity diminution at 476 nm with growing $C_4MIm^+Cl^-$ concentration. Adapted with permission from Ref. [34], copyright (2009) American Chemical Society.

**Table 1.** Dimensions of β-cyclodextrins (β-CD), sulfobutylether β-cyclodextrin($SBE_7βCD$), cucurbit[7]uril (CB7), and *p*-sulfonatocalix[6]arene (SCX6)

| Macrocycle (host) | Internal diameter (nm) | External diameter (nm) | Height (nm) |
|---|---|---|---|
| β-CD[a] | 0.6–0.65 | 1.54 | 0.79 |
| $SBE_7βCD$[a] | 0.6–0.65 | 1.54 | – |
| SCX6[b] | 0.76 | 0.496 | 1.624 |
| CB7[c] | 0.73 | 0.54 | 0.91 |

[a,b,c]Taken from References 37, 70, 57, respectively.

**Table 2.** Binding constants of certain cation binding to CB7 in water at 296 K. Adapted with permission from Ref. [34], copyright (2009) American Chemical Society

| Host compound | $K$ ($M^{-1}$) |
|---|---|
| $C_1MIm^+(CH_3O)_2PO_2^-$ | $7.5\times10^4$ |
| $C_2MIm^+Cl^-$ | $1.8\times10^5$ |
| $C_3MIm+Br^-$ | $1.9\times106$ |
| $C_4MIm+Cl^-$ | $6.7\times10^6$ |
| $C_4MIm^+Br^-$ | $6.3\times10^6$ |
| $C_4MIm^+BF_4^-$ | $7.6\times10^6$ |
| $C_4MIm^+PF_6^-$ | $7.6\times10^6$ |
| $C_4MP^+Cl^-$ | $3.6\times10^7$ |
| $C_6MIm^+Cl^-$ | $2.0\times10^7$ |
| $C_6MIm^+Br^-$ | $1.9\times10^7$ |
| $C_8MIm^+Cl^-$ | $8.9\times10^6$ |
| $C_8MIm^+Br^-$ | $8.3\times10^6$ |
| $C_9MIm^+Br^-$ | $5.3\times10^6$ |
| $C_{10}MIm^+Br^-$ | $2.9\times10^6$ |
| $C_{12}TA^+Br^-$ | $2.8\times10^6$ |
| $C_{12}MIm^+Br^-$ | $8.5\times10^5$ |
| $C_{12}Py^+Br^-$ | $8.0\times10^5$ |
| $C_{14}MIm^+Br^-$ | $5.9\times10^5$ |
| Dopamine·HCl | $1.0\times10^5$ |
| Berberine$^+Cl^-$ | $1.6\times10^6$ |
| DAPI | $1.1\times10^7$ |

ing interaction among the guests for CB7, eventually displacing DAPI guest by $C_4MIm^+$. On the other hand, the above competing interaction by DAPI and $C_4MIm$ for the CB7 cavity was used to evaluate the binding constant for the $C_4MIm^+$-CB7 interaction. Interestingly, it was observed that the $K_{eq}$ for the $CnMIm^+$-CB7 interaction altered considerably on changing the length of the alkyl substituent and the $K_{eq}$ estimated for diverse systems are presented in Table 2[34]. The $K_{eq}$ values decreased by more than 2 orders when the side chain was made smaller (hexyl to methyl). However, the increase in length of the side chain moiety negatively affected the $K_{eq}$ only to smaller extent[34]. Explicitly, the $C_6MIm^+$ IL displayed the most stable interaction with CB7.

The observation that $C_6MIm^+$ has better interaction with the CB7 moiety is quite likely that the cationic methyl imidazolium head group gets into the CB7 portal. With the increase in the carbon atoms from $C_1MIm^+$ in the aliphatic chain, the hydrophobic influence with the CB7 interior increases as seen from the binding values going from $C_1MIm^+$-CB7 to $C_6MIm^+$-CB7[34]. Beyond this optimum values, addi-

tional increase in the chain length, destabilizes the binding due to the non-confinement of the added alkyl chains. At the same time, Table 2 also addresses to the concern that there is not much effect of anions. This is reasonable to understand as the negatively charged CB7 portals would naturally dislike the interaction with the anions.

Further, the variations in the binding interaction with the changes in the head groups have also been analyzed using different surfactants having a dodecyl group. As seen from Table 2, the binding values got decreased in the order dodecyl trimethyl ammonium ($C_{12}TA^+$) > $C_{12}MIm^+$ > dodecyl pyridinium cations. These variations, in other words, proposes that the increasing hydrophobicity of the head group plays a decisive role. The smaller trimethyl ammonium head is more hydrophilic than the heterocyclic pyridinium nitrogens and makes methyl imidazolium less hydrophobic than pyridinium. With butyl derivatives, the more hydrophilic cation of $C_4MP^+Cl^-$ having a quaternary nitrogen linked to aliphatic and cyclo-aliphatic moieties renders better stability complexes than $C_4MIm^+Cl^-$, in which the cationic charge is dispersed in the heterocyclic ring[34]. Overall, the effect of aliphatic chain length influence the binding to a larger extend than the changes in the head groups[34]. Attention must be given to the presence of $Na^+$ ions present in the buffer solutions as they get coordinated readily with the CB7 portals, affecting the binding of the desired guest.

*2.3.3. Competitive binding of CB7-DAPI complex with compounds of biological importance (dopamine, tyrosine and berberine):*

To elucidate the usage of DAPI-CB7 complex for the detection of biological analytes, the interaction of dopamine hydrochloride (DOPA·HCl) with the CB7-DAPI complex has been explored. As envisaged, incremental addition of DOPA·HCl resulted in changes in the absorption/fluorescence features established for the CB7-DAPI complex. The changes were also similar to that observed with the addition ionic liquids discussed above and corresponds to the competitive interaction of the added analyte displacing the bound DAPI[34]. The binding constant was found to be $1.0\times10^5$ $M^{-1}$. This value is found to be in the range of $K = 2.33\times10^5$ $M^{-1}$ documented for tyrosine hydrochloride (Tyr) with CB7[80]. In addition to DOPA and Tyr, competitive inclusion of Berberine chloride (B), a clinically important natural isoquinoline alkaloid, against DAPI-CB7 interaction was examined. Berberine cation ($B^+$) present very strong interaction with CB7 forming a 1:1 inclusion having $K = 1.6\times10^6$ $M^{-1}$ with ~500-fold increase in the emission intensity[81]. Since $B^+$ absorption band in water extend up to ~480 nm, selective excitation of $B^+$ is convenient in the presence of DAPI also. On titration of the CB7-$B^+$ solution with DAPI, the strong emission intensity from the CB7:$B^+$ complex ($\phi_f$ 0.26)[81] steadily decreased with increasing DAPI. The changes apparently corresponded to the competitive displacement of $B^+$ from the CB7 cavity. The competitive titration data has been analyzed to extract the binding constant of CB7 with DAPI by using the known value of CB7 with $B^+$. The analysis rendered $K_{DAPI}$ for CB7-DAPI as $1.0\times10^7$ $M^{-1}$ and is in perfect match with the binding constant evaluated independently in a direct measurement (*vide supra*)[34].

## Conclusions

This review article discusses the host-guest complex formation of 4′,6-diamidino-2-phenylindole (DAPI) in aqueous solution with cavitand hosts; cucurbit[7]uril (CB7), *p*-sulfonatocalix[6]arene (SCX6) and sulfobutylether β-cyclodextrin ($SBE_7\beta CD$). The significant modulations observed in the absorption/fluorescence and other spectroscopic characteristics of DAPI were ascribed to the formation of stable 1:1 inclusion complex with these host molecules and were found to be distinctly different with each host molecules. The $K_{eq}$ values estimated from the absorption/fluorescence titrations are in the range of ~$10^7$ $M^{-1}$ for CB7-DAPI system, ~$10^6$ $M^{-1}$ for SCX6-DAPI and ~$10^5$ $M^{-1}$ for $SBE_7\beta CD$-DAPI systems and are in accordance with the portal group features of the individual hosts. In case of SCX6-DAPI and $SBE_7\beta CD$-DAPI systems, where the DAPI emission got quenched due to complexation, stimuli-responsive fluorescence regeneration of DAPI was achieved by metal ions/competitive binders such as ionic liquids, surfactants, adamantylamine (AD), and biologically important compound, dopamine/berberine through competitive binding with the host molecules. These competitive binding responses are crucial to measures for designing controlled drug delivery through supramolecular approaches. In case of SCX6-DAPI system, the SCX6 induced emission changes with change in pH is worthy as on-off fluorescence switch. This system also offers as a good optical probe for the facile evaluation of the $pK_a$ of SCX host by emission measurements.

**Acknowledgements**

The authors acknowledge all the contributed authors and collaborators of our published works cited here. We also acknowledge the constant support and encouragement of Dr. Awadhesh Kumar, Head, Radiation & Photochemistry Division, BARC, India.

**References**

1. S. Dutta Choudhury, J. Mohanty, H. Pal and A. C. Bhasikuttan, *J. Am. Chem. Soc.*, 2010, **132**, 1395.
2. W. M. Nau, G. Ghale, A. Hennig, H. Bakirci and D. M. Bailey, *J. Am. Chem. Soc.,* 2009, **131**, 11558.
3. F. Perret, A. N. Lazar and A. W. Coleman, *Chem. Commun.,* 2006, 2425.
4. H. Bakirci and W. M. Nau, *Adv. Funct. Mater.,* 2006, **16**, 237.
5. R. Khurana, S. Agarwalla, G. Sridhar, N. Barooah, A. C. Bhasikuttan and J. Mohanty, *ChemPhysChem.,* 2018, **19**, 2349.
6. J. Mohanty, K. Jagtap, A. K. Ray, W. M. Nau and H. Pal, *ChemPhysChem.,* 2010, **11**, 3333.
7. M. Shaikh, J. Mohanty, A. C. Bhasikuttan, V. D. Uzunova, W. M. Nau and H. Pal, *Chem. Commun.,* 2008, 3681.
8. R. Khurana, N. Barooah, A. C. Bhasikuttan and J. Mohanty, *Org. Biomol. Chem.,* 2017, **15**, 8448.
9. J. Mohanty, S. Dutta Choudhury, H. P. Upadhyaya, A. C. Bhasikuttan and H. Pal, *Chem. Eur. J.,* 2009, **15**, 5215.
10. R. Wang, L. Yuan and D. H. Macartney, *Chem. Commun.,* 2005, 5867.
11. B. C. Pemberton, N. Barooah, D. K. Srivatsava and J. Sivaguru, *Chem. Commun.,* 2010, **46**, 225.
12. S. Dutta Choudhury, J. Mohanty, H. P. Upadhyaya, A. C. Bhasikuttan and H. Pal, *J. Phys. Chem. B,* 2009, **113**, 1891.
13. N. Barooah, A. C. Bhasikuttan, V. Sudarsan, S. Dutta Choudhury, H. Pal and J. Mohanty, *Chem. Commun.,* 2011, **47**, 9182.
14. R. N. Dsouza, U. Pischel and W. M. Nau, *Chem. Rev.,* 2011, **111**, 7941.
15. J. Lagona, P. Mukhopadhyay, S. Chakrabarti and L. Isaacs, *Angew. Chem. Int. Ed.,* 2005, **44**, 4844.
16. A. C. Bhasikuttan, H. Pal and J. Mohanty, *Chem. Commun.,* 2011, **47**, 9959.
17. J. Mohanty and W. M. Nau, *Angew. Chem. Int. Ed.,* 2005, **44**, 3750.
18. W. M. Nau and J. Mohanty, *Int. J. Photoenergy,* 2005, **7**, 133.
19. A. C. Bhasikuttan, S. Dutta Choudhury, H. Pal and J. Mohanty, *Isr. J. Chem.,* 2011, **51**, 634.
20. M. N. Shinde, S. Dutta Choudhury, N. Barooah, H. Pal, A. C. Bhasikuttan and J. Mohanty, *J. Phys. Chem. B,* 2015, **119**, 3815.
21. M. N. Shinde, A. C. Bhasikuttana and J. Mohanty, *Supramol. Chem.,* 2016, **28**, 517.
22. X. Li, B.-Y. Zheng, M.-R. Ke, Y. Zhang, J.-D. Huang and J. Yoon, *Theranostics,* 2017, **7**, 2746.
23. J. Mohanty, A. C. Bhasikuttan, S. Dutta Choudhury and H. Pal, *J. Phys. Chem. B (Letts.),* 2008, **112**, 10782.
24. J. Mohanty, H. Pal, A. K. Ray, S. Kumar and W. M. Nau, *ChemPhysChem.,* 2007, **8**, 54.
25. D. Banerjee and S. K. Pal, *J. Phys. Chem. B,* 2008, **112**, 1016.
26. A. Mazzini, P. Cavatorta, M. Iori, R. Favilla and G. Sartor, *Biophys. Chem.,* 1992, **42**, 101.
27. D. Banerjee, S. K. Srivastava and S. K. Pal, *J. Phys. Chem. B,* 2008, **112**, 1828.
28. F. A. Tanious, J. M. Veal, H. Buczak, L. S. Ratmeyer and W. D. Wilson, *Biochemistry,* 1992, **31**, 3103.
29. D. Vlieghe, J. Sponer and L. V. Meervelt, *Biochemisty,* 1999, **38**, 16443.
30. A. G. Szabo, D. T. Krajcarski, P. Cavatorta, L. Masotti and M. L. Barcellona, *Photochem. Photobiol.,* 1986, **44**, 143.
31. M. L. Barcellona and E. Gratton, *Biophys. Chem.,* 1991, **40**, 223.
32. J. Kapuscinski, *Biotechnic & Histochem.,* 1995, **70**, 220.
33. M. N. Shinde, A. C. Bhasikuttan and J. Mohanty, *ChemPhysChem.,* 2015, **16**, 3425.
34. Z. Miskolczy, L. Biczok, M. Megyesi and I. Jablonkai, *J. Phys. Chem. B,* 2009, **113**, 1645.
35. (a) J. Mohanty, S. Dutta Choudhury, N. Barooah, H. Pal and A. C. Bhasikuttan in: "Mechanistic Aspects of Host-Guest Binding in Cucurbiturils: Physicochemical Properties", Vol. 1, eds. G. W. Gokel and J. L. Atwood, Elsevier, Amsterdam, 2017, 435; (b) J. Mohanty, R. Khurana, N. Barooah and A. C, Bhasikuttan, *J. Indian Chem. Soc*., 2018, **95**, 533.
36. T. Loftsson, P. Jarho, M. Másson and T. Järvinen, *Expert Opin. Drug Deliv.,* 2005, **2**, 335.
37. R. Khurana, J. Mohanty, N. Padma, N. Barooah and A. C. Bhasikuttan, *Chem. Eur. J.,* 2019, **25**, 13939.
38. J. Szejtli, *Chem. Rev.,* 1998, **98**, 1743.
39. K. N. Houk, A. G. Leach, S. P. Kim and X. Zhang, *Angew. Chem. Int. Ed.,* 2003, **42**, 4872.
40. A. S. Jain, A. A. Date, R. R. S. Pissurlenkar, E. C. Coutinho and M. S. Nagarsenker, *AAPS Pharm. Sci. Tech.,* 2011, **12**, 1163.
41. V. J. Stella, "Proceedings of the Eighth International Symposium on Cyclodextrins", 1996, 471-476.
42. M. N. Shinde, R. Khurana, N. Barooah, A. C. Bhasikuttan and J. Mohanty, *J. Phys. Chem. C,* 2017, **121**, 20057.
43. R. Khurana, A. S. Kakatkar, S. Chatterjee, N. Barooah, A. Kunwar, A. C. Bhasikuttan and J. Mohanty, *Front. Chem.,* 2019, **7**, 452(1-11).

44. R. Khurana, N. Barooah, A. C. Bhasikuttan and J. Mohanty, *ChemPhysChem.,* 2019, **20**, 2498.
45. V. Kadam, A. S. Kakatkar, N. Barooah, S. Chatterjee, A. C. Bhasikuttan and J. Mohanty, *RSC Adv.,* 2020, **10**, 25370.
46. C. D. Gutsche, "Calixarenes Revisited In Monographs in Supramolecular Chemistry", The Royal Society of Chemistry, Cambridge, 1998.
47. S. Shinkai, S. Mori, H. Koreishi, T. Tsubaki and O. Manabe, *J. Am. Chem. Soc.,* 1986, **108**, 2409.
48. H. Bakirci, T. Schwarzlose, A. L. Koner and W. M. Nau, *Chem. Eur. J.,* 2006, **12**, 4799.
49. R. V. Rodik, V. I. Boyko, V. I. Kalchenko, *Cur. Med. Chem.,* 2009, **16**, 1630.
50. M. N. Shinde, N. Barooah, A. C. Bhasikuttan, J. Mohanty, *Chem. Commun.,* 2016, **52**, 2992.
51. A. Jadhav, V. S. Kalyani, N. Barooah, D. D. Malkhede and J. Mohanty, *ChemPhysChem.,* 2015, **16**, 420.
52. V. S. Kalyani, D. D. Malkhede and J. Mohanty, *Phys. Chem. Chem. Phys.,* 2017, **19**, 21382.
53. C. Mehra, R. Gala, A. Kakatkar, V. Kumar, R. Khurana, S. Chatterjee, N. N. Kumar, N. Barooah, A. C. Bhasikuttan and J. Mohanty, *Chem. Commun.,* 2019, **55**, 14275.
54. M. N. Shinde, R. Khurana, N. Barooah, A. C. Bhasikuttan and J. Mohanty, *Org. Biomol. Chem.,* 2017, **15**, 3975.
55. E. Masson, X. Ling, R. Joseph, L. Kyeremeh-Mensah and X. Lu, *RSC Adv.,* 2012, **2**, 1213.
56. K. I. Assaf and W. M. Nau, *Chem. Soc. Rev.,* 2015, **44**, 394.
57. J. W. Lee, S. Samal, N. Selvapalam, H.-J. Kim and K. Kim, *Acc. Chem. Res.,* 2003, **36**, 621.
58. T. Goel, N. Barooah, M. B. Mallia, A. C. Bhasikuttan and J. Mohanty, *Chem. Commun.,* 2016, **52**, 7306.
59. A. E. Kaifer, W. Li and S. Yi, *Isr. J. Chem.,* 2011, **51**, 496.
60. V. D. Uzunova, C. Cullinane, K. Brix, W. M. Nau and A. I. Day, *Org. Biomol. Chem.,* 2010, **8**, 2037.
61. R. Oun, R. S. Floriano, L. Isaacs, E. G. Rowan and N. J. Wheate, *Toxicol. Res.,* 2014, **3**, 447.
62. S. J. Barrow, S. Kasera, M. J. Rowland, J. D. Barrio and O. A. Scherman, *Chem. Rev.,* 2015, **115**, 12320.
63. G. Ghale and W. M. Nau, *Acc. Chem. Res.,* 2014, **47**, 2150.
64. J. Mohanty, N. Thakur, S. Dutta Choudhury, N. Barooah, H. Pal and A. C. Bhasikuttan, *J. Phys. Chem. B,* 2012, **116**, 130.
65. N. Barooah, J. Mohanty, H. Pal and A. C. Bhasikuttan, *Proc. Natn. Acad. Sci., India,* 2014, **84**, 1.
66. I. Ghosh and W. M. Nau, *Adv. Drug Deliv. Rev.,* 2012, **64**, 764.
67. T.-C. Lee and O. A. Scherman, *Chem. Commun.,* 2010, **46**, 2438.
68. S. Gurbuz, M. Idris and D. Tuncel, *Org. Biomol. Chem.,* 2015, **13**, 330.
69. M. Shaikh, J. Mohanty, A. C. Bhasikuttan and H. Pal, *J. Spectrosc. Dyn.,* 2012, **2:1**, 1.
70. C. D. Gutsche, "Calixarenes: An Introduction", Royal Society of Chemistry, Cambridge, 2008.
71. J. Mohanty, H. Pal, S. K. Nayak, S. Chattopadhyay and A. V. Sapre, *J. Chem. Phys.,* 2002, **117**, 10744-10751.
72. J. Mohanty, H. Pal, S. K. Nayak, S. Chattopadhyay and A. V. Sapre, *Chem. Phys. Lett.,* 2003, **370**, 641.
73. K. Lang, P. Kubat, P. Lhotak, J. Mosinger and D. M. Wagnerova, *Photochem. Photobiol.,* 2001, **74**, 558.
74. M. Shaikh, J. Mohanty, D. K. Maity, S. K. Nayak and H. Pal, *J. Photochem. Photobiol. A: Chemistry,* 2008, **195**, 116.
75. J. Mohanty, A. C. Bhasikuttan, W. M. Nau and H. Pal, *J. Phys. Chem. B,* 2006, **110**, 5132.
76. T. Pedzinski, B. Marciniak and G. L. Hugb, *J. Photochem. Photobiol. A,* 2002, **150**, 21.
77. B. Valeur, in: "Molecular Fluorescence Principles and Applications", Wiley-VCH, 2002, 147.
78. H. Rene, A. Lene and S. Claus, *Results in Pharma Sciences,* 2011, 57.
79. M. L. Barcellona and E. Gratton, *Eur. Biophys. J.,* 1990, **17**, 315.
80. H. Cong, L.-L. Tao, Y.-H. Yu, F. Yang, Y. Du, Z. Tao and S.-F. Xue, *Asian J. Chem.,* 2007, **19**, 961.
81. M. Megyesi, L. Biczo´k and I. Jablonkai, *J. Phys. Chem. C,* 2008, **112**, 3410.